INTERNATIONAL JOURNAL OF LATEST TECHNOLOGY IN ENGINEERING, MANAGEMENT & APPLIED SCIENCE (IJLTEMAS)
ISSN 2278-2540 | DOI: 10.51583/IJLTEMAS | Volume XV, Issue VIII, August 2026

Spray-Pyrolyzed Aluminium-Doped Zinc Oxide Thin Films for Transparent Conducting Applications

S. G. Ibrahim[1*], D. S. Dhote[2]

[1] Department of Physics, Prof. Ram Meghe College of Engineering & Management, Badnera-444701, Maharashtra, India

[2] Department of Electronics, Brijlal Biyani Science College, Amravati-444601, Maharashtra, India

DOI: https://doi.org/10.51583/IJLTEMAS.2026.150800038

Received: 11 August 2026; Accepted: 18 August 2026; Published: 07 September 2026

ABSTRACT

Aluminium doped zinc oxide (AZO) thin films were produced by spray pyrolysis on glass substrates at the substrate temperature of 573 K and the X-ray diffraction analysis confirmed the nanocrystalline nature of the film with a hexagonal wurtzite structure and (002) preferred orientation. Surface morphology reveals that the deposited film is uniformly distributed over the glass substrate with absence of any voids or cracks. The optical band gap (Eg) of the AZO films was found to be 3.32 eV, the resistivity (ρ) of the AZO films was of the order of 4.21×10^{-3} Ω cm and the transmittance reaching maximum value of 80.17%, which is reasonably good and desirable for transparent conducting oxide applications.

Keywords: Spray pyrolysis; Thin films; Transparent conducting oxide; Optical properties; Electrical properties; Optoelectronic devices

Corresponding Author: Dr. S. G. Ibrahim (ibrahim.ghause@gmail.com)

INTRODUCTION

ZnO, the hexagonal wurtzite structure zinc oxide semiconductor, has interesting optical, electrical and piezoelectric properties, while being a wide band gap semiconductor. It is highly transparent in the visible spectrum, chemically stable and has tuneable electrical conductivity and has thus been the subject of much interest in other applications like solar cells, transparent electrodes, light emitting devices, thin-film transistors, sensors and other optoelectronic devices [1–15]. The electrical conductivity of undoped ZnO is, however, relatively low for many applications of transparent electrodes, and is highly sensitive to intrinsic defects and non-stoichiometry. Thus, controlled doping has been extensively studied for the improvement of its electrical properties without sacrificing the high optical transparency.

In the various dopants used for the ZnO, Al-doped ZnO (AZO) is attractive due to its high electrical conductivity, the ability of being transparent in the visible range and low material cost, non-toxicity and elemental abundance. The incorporation of Al into the ZnO lattice may affect the carrier concentration, crystallinity, optical band gap and electrical transport characteristics of the semiconductor [17, 18]. The properties of AZO render it a promising alternative to the traditional transparent conducting oxides like indium tin oxide and fluorine doped tin oxide [19–24] without using indium. The high optical transmission and sufficiently low electrical resistivity is especially significant for the transparent conducting applications, which however is strongly dependent on Al concentration, deposition conditions, microstructure and post deposition treatment.

Thin films of AZO have been produced by various physical and chemical deposition methods. For the Al doped ZnO, films prepared by RF magnetron sputtering were highly conducting and transparent by Jayaraj et al. [25] and the films prepared from SILAR technique by Mondal et al. [26] showed improved c-axis orientation and low resistivity after the Al was incorporated in the films. The effects of annealing temperature

ISSN 2278-2540 | DOI: 10.51583/IJLTEMAS | Volume XV, Issue VIII, August 2026

on the crystallisation and physical properties of AZO nanoparticles were reported by Chen et al. [27] while the effects of Al doping on the optical and electrical properties of spray-pyrolysed ZnO films were reported by Alaeddine et al. [28]. The ability of AZO to detect humidity, CO, flexible pressure sensors, and thin-film solar cells transparent electrodes has been demonstrated in other studies [29–32]. These investigations show the versatility of AZO but also suggest that its properties are very much dependent on the route of synthesis and the processing parameters.

The spray pyrolysis is of particular interest among the deposition methods, due to the ease of the experimental set-up of the process, its relatively low equipment investment, simple compositional control and the possibility of large area coating. Kaid and Ashour [33] spray pyrolysed AZO films on glass, and found that the ZnO films were polycrystalline hexagonal films with visible transmittance 90%–95% and optical band-gap values of 3.30–3.55 eV, which depends on the thickness of the film. Ambedkar et al. [34] studied the effect of Al concentration on spray-pyrolysed AZO films and found the preferential growth of (002) planes, along with the significant variation in the morphology, optical band gap, lattice strain and thermoelectric properties. Hazmin et al. [35] have investigated low-temperature spray deposition of AZO on Teflon substrate and showed that the spray parameters affect the structural and optical properties. AL-Arique et al [36] recently studied the effect of annealing temperature on the crystallite size and surface morphology for ZnO and AZO films on glass, and observed variations in the optical transmittance and band gap.

Although these investigations have been performed, it is still essential to find a proper crystallinity–optical transparency–electrical conductivity compromise with a simple and economic spray-pyrolysis process for the development of AZO as a transparent conducting oxide without indium. So far, most of the studies have focused on single processing parameters that include Al concentration, substrate temperature, spray process parameters, and film thickness or annealing process after the deposition [28, 33-36]. These parameters can affect the crystallographic orientation, crystallite properties, surface morphology, optical absorption and charge transport simultaneously, and the interrelationships among these must be further investigated under defined deposition conditions. For this reason, a comprehensive characterization of the structural, morphological, optical and electrical properties of AZO growth on glass at moderate substrate temperatures could be useful to evaluate the possibility of using AZO as a transparent conducting material.

Thus, the present work examines the deposition of AZO thin films with spray pyrolysis at 573 K on glass substrates. The study illustrates the relationship between structural and morphological properties of the deposited film and its optical and electrical properties focusing on crystallographic orientation, surface morphology, optical transmittance, optical band gap and electrical resistivity. The prepared film has a hexagonal wurtzite structure with a preferentially orientation, which is compact granular morphology, optical band gap of 3.32 eV, maximum optical transmittance of about 80.17±0.92% and electrical resistivity of 4.21×10^{-3} Ωcm. The two parameters analyzed together give an idea of the feasibility of spray-pyrolysed AZO as a cost-effective and indium-free transparent conducting material for optoelectronic applications.

Experimental details

The zinc acetate dihydrate ($Zn(CH_3COO)_2\cdot 2H_2O$) was used as a source of zinc oxide (ZnO) compound, aluminium nitrate nonahydrate ($Al(NO_3)_3\cdot 9H_2O$) was used as a source of aluminium as a dopant, methanol (CH_3OH) was used as a solvent, and double distilled water was used to clean glass slides used in the ultrasonic bath.

A solution of zinc acetate was obtained by dissolving 0.2 M of zinc acetate dihydrate in methanol. The solution was stirred for 20 min at room temperature. The substrate temperature was kept at 573K (± 5K), spray rate 5mL/min, distance between nozzle and substrate 30cm with nozzle diameter of 0.5mm. The correct quantity of aluminium nitrate was added to obtain 1at% Al doping in ZnO.

The gravimetric method was used for measuring the thin film thickness of the deposited film [37]. The deposited aluminium doped zinc oxide thin films were analysed by using X-ray diffractometer (Philips PW 1710) with Cu Kα radiation of wavelength 1.5405 Å. A JOEL 6380A was utilized for obtaining scanning

ISSN 2278-2540 | DOI: 10.51583/IJLTEMAS | Volume XV, Issue VIII, August 2026

electron microscopy data of the films. The Lambda 25 UV-Vis spectrophotometer (PerkinElmer) was used for optical absorption studies at normal incidence between the wavelengths of 300-950 nm. The electrical resistivity of the films was measured by the two-point probe method in the temperature range of 303-513K and the films were found to be dark. Thermo-emf voltage was measured across the film to determine the type of conductivity of aluminium doped zinc oxide thin film.

RESULTS AND DISCUSSION

4.1 Structural Studies

The X-ray diffraction pattern of AZO thin film (Figure 1), grown at 573K is polycrystalline hexagonal wurtzite.

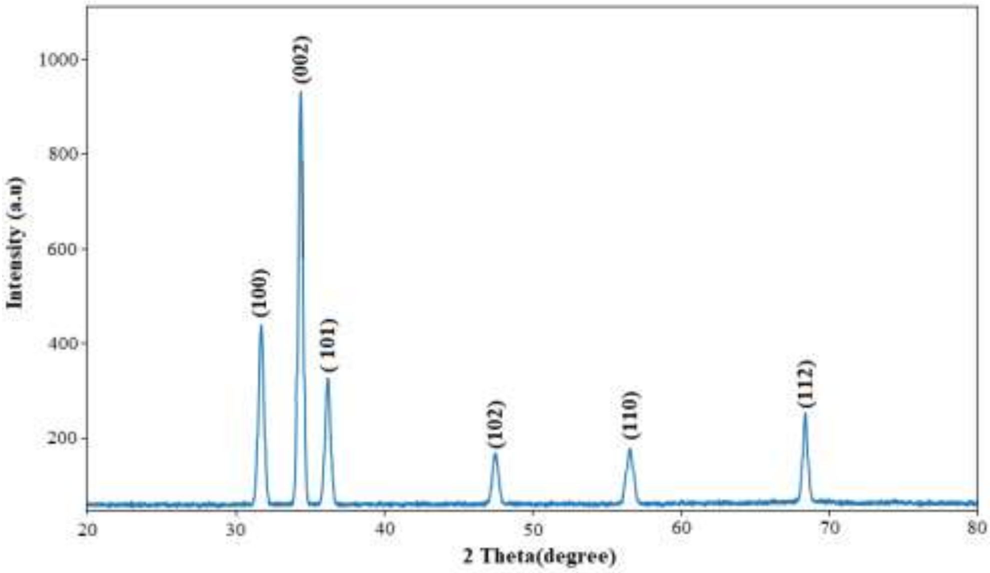

Figure 1: XRD pattern of aluminium doped zinc oxide thin films

The major diffraction peaks are seen at 31.748°, 34.518° and 36.362°, representing the (100), (002) and (101) crystallographic planes, respectively. In these reflections the (002) peak is the strongest, suggesting preferential orientation of the crystallites in the c-axis direction.

Table 1: Comparison of observed and standard XRD data of AZO thin films (JCPDS card 36-1451)

Film	Observed data		Standard data		h k l	phase
	2θ (degree)	d (Å)	2θ (degree)	d (Å)		
AZO	31.748	2.821	31.770	2.814	1 0 0	Hexagonal
	34.518	2.591	34.422	2.603	0 0 2	Hexagonal
	36.362	2.329	36.253	2.476	1 0 1	Hexagonal
	47.560	1.890	47.539	1.911	1 0 2	Hexagonal
	56.680	1.611	56.600	1.625	1 1 0	Hexagonal
	67.898	1.361	67.960	1.358	1 1 2	Hexagonal

ISSN 2278-2540 | DOI: 10.51583/IJLTEMAS | Volume XV, Issue VIII, August 2026

Other diffraction peaks, at higher diffraction angles, are also seen for the (102), (110) and (112) planes at 47.560°, 56.680° and 67.898°, further confirming the formation of the wurtzite ZnO structure. In this representative pattern, the additional prominent peaks of secondary phases are not taken into consideration indicating a single-phase structure of AZO. The strong (002) orientation may be due to the growth of ZnO crystallites which favor the (002) crystal plane under the spray-pyrolysis conditions. The crystallite size was found to be 21.9 nm by using FWHM data and Debye Scherer's formula [37].

$$d = \frac{K\lambda}{\beta \cos\theta} \qquad (1)$$

The shape factor 'K'' is equal to 0.94, β is the angular line width at half maximum intensity, θ is the Bragg's angle and λ is the wavelength used.

4.2 Surface Morphology Studies

Spray Pyrolyzed AZO thin films were investigated using scanning electron microscopy (SEM). The SEM image (Figure 2), shows a uniform and dense surface structure with an even layer of material covering the substrate.

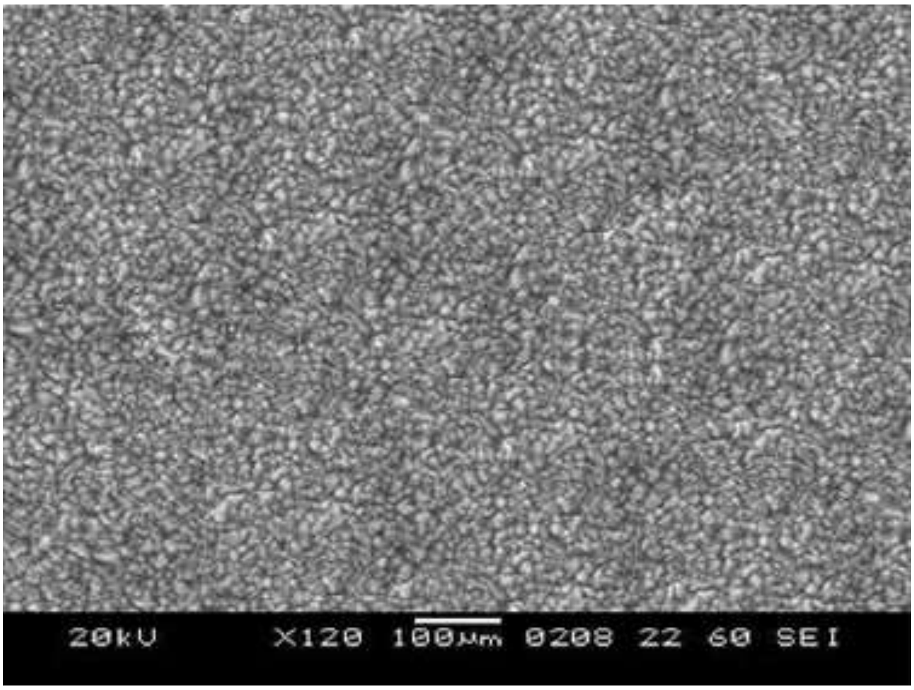

Figure 2: SEM image of aluminium doped zinc oxide thin films

The film is composed of uniformly distributed fine grains which are tightly packed and are continuous over the surface. There are no cracks, pinholes or voids observed, which suggests high quality film and strong adhesion to the glass substrate. The uniform grain distribution indicates good nucleation and growth in the spray pyrolysis process, which means the microstructure is dense. This small morphology is advantageous for minimizing carrier scattering at grain boundaries and increasing electrical conductivity while retaining good optical transparency needed for transparent conducting oxide applications.

4.3 Electrical Studies

Electrical properties of the AZO thin films were studied via I–V and temperature dependent resistivity measurements. The current increases with the applied voltage with an approximately linear I–V response suggesting a predominantly ohmic response, as illustrated in Figure 3. The resistivity of AZO film was 4.12×10^{-3} Ωcm. This relatively low resistivity may be explained by the introduction of Al^{3+} ions into the lattice of ZnO which gives additional charge carriers and thus improves the conductivity.

ISSN 2278-2540 | DOI: 10.51583/IJLTEMAS | Volume XV, Issue VIII, August 2026

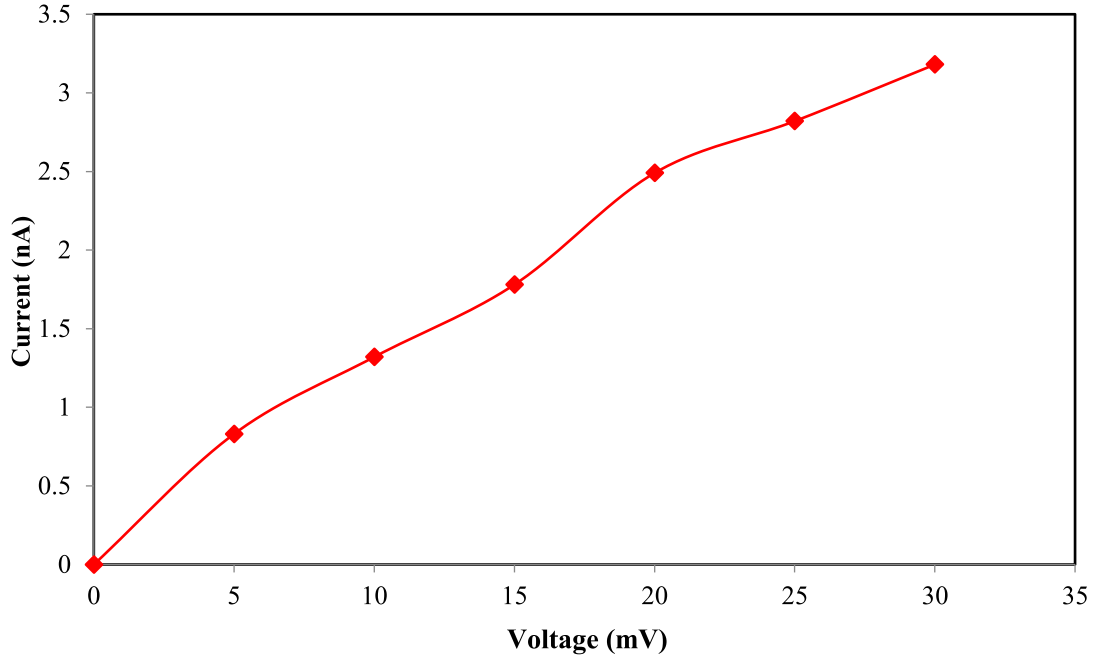

Figure 3: I-V characteristic of aluminium doped zinc oxide thin films

The resistivity is calculated using the formula,

$$\rho = \rho_o e^{\frac{Ea}{KT}} \quad (2)$$

where 'ρ' is the electrical resistivity. 'ρ_o' is a constant, 'K' is the Boltzmann constant (1.38×10^{-23} J/k) and 'Ea' is the activation energy needed for conduction.

The variation of logρ with 1/T is shown in the figure 4, which shows that, logρ decreases with increasing 1/T which means that resistivity decreases with temperature. This is also a negative temperature coefficient of resistivity which confirms the semiconducting nature of the AZO film and indicates thermally activated charge transport.

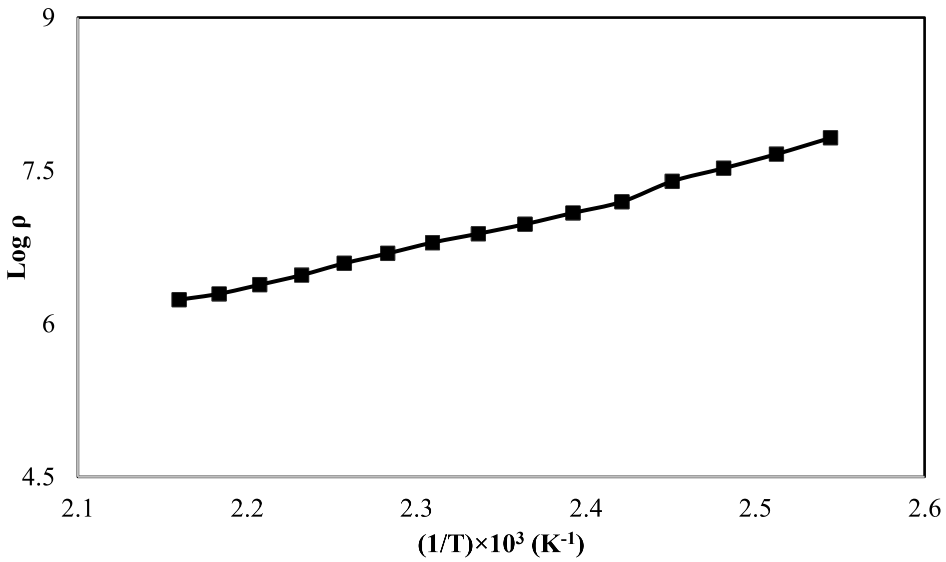

Figure 4: Variation of Log of resistivity with 1/T of aluminium doped zinc oxide thin films

The relatively low electrical resistivity with high optical transparency indicates the promising AZO films as transparent conducting materials for optoelectronic applications.

ISSN 2278-2540 | DOI: 10.51583/IJLTEMAS | Volume XV, Issue VIII, August 2026

4.4 Thermo-emf Studies

The experimental results indicate almost monotonic increase of thermo-emf with temperature. The thermo-emf increases relatively slowly at low temperatures (303–400 K), and sharply above about 400 K. The temperature dependent charge transport characteristics of the AZO thin film were examined by performing thermo-emf studies (Figure 5). The thermo-emf of cells increased with temperature from 0.22eV at 303 K to 6.23eV at 483 K, which shows that the response of thermoelectric response increases with temperature.

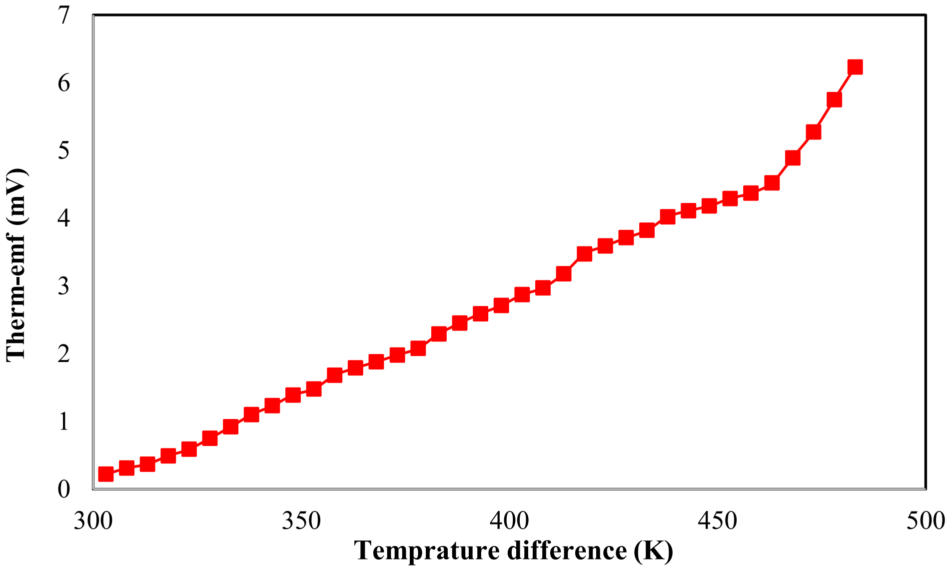

Figure 5: Variation of thermo-emf (mV) with temperature difference of aluminium doped zinc oxide thin films

The almost linear relationship of thermo-emf vs temperature having an R^2 nearly close to 0.985 implies there is a strong temperature dependent response to thermoelectric response. An Arrhenius plot was used to estimate the activation energy. The activation energy value obtained from the slope of the fitted linear region was around 0.198eV (≈ 0.20 eV), which showed that the charge-carrier transport in the AZO film was thermally activated.

4.5 Optical Studies

The aluminium doped zinc oxide thin film was studied in the wavelength range of 300-950 nm for its optical absorption properties.

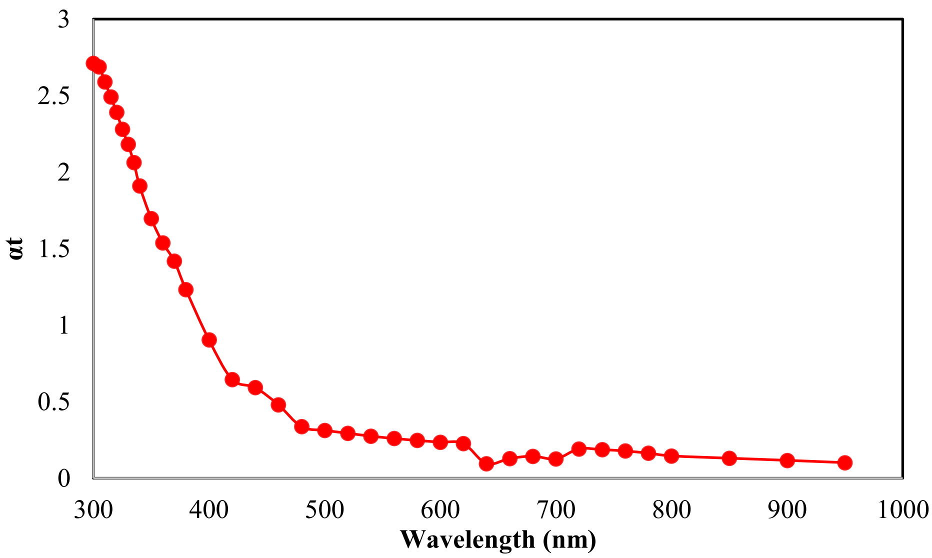

Figure 6: Variation of optical absorption vs. wavelength of aluminium doped zinc oxide thin films

ISSN 2278-2540 | DOI: 10.51583/IJLTEMAS | Volume XV, Issue VIII, August 2026

The absorption coefficient was strongly wavelength dependent and reached a maximum value of ~2.7 in the near-UV. From 420 nm to longer wavelengths, the absorption coefficient did not increase significantly, and was as small as ~0.10 at ~640 nm. The increased absorption in the UV region is due to the basic electronic transitions occurring near the absorption edge, and the drop in absorption in the visible region is in line with the excellent optical transparency of the AZO films.

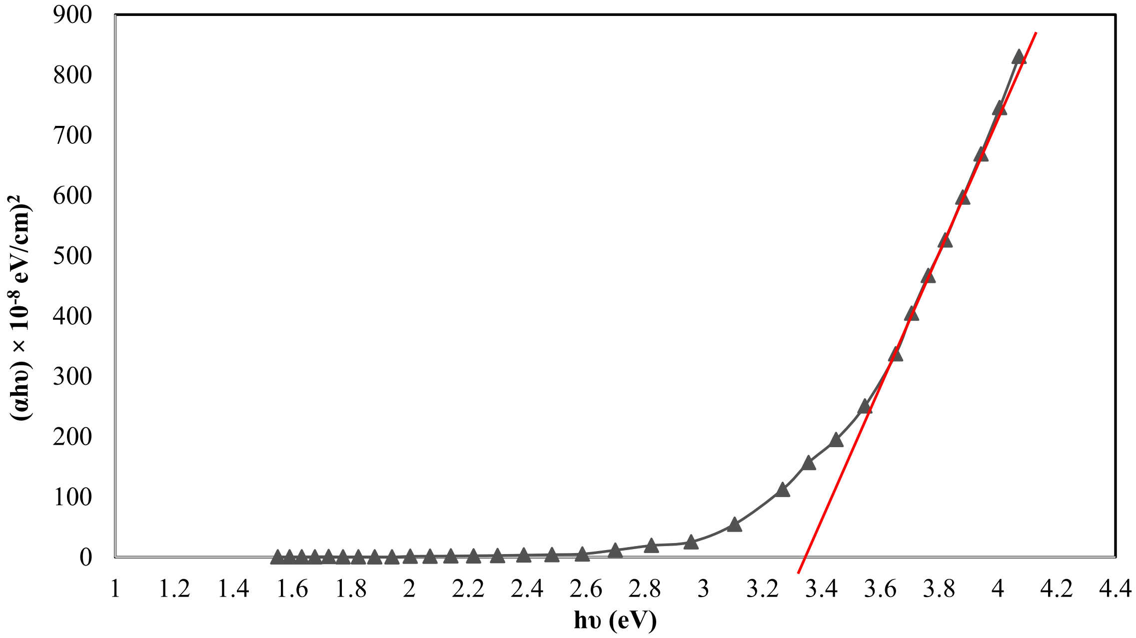

Figure 7: The plots of $(\alpha h\upsilon)^2$ vs. hυ of deposited aluminium doped zinc oxide thin films

The variation of the optical absorption parameter (αt) with wavelength is shown in Figure 6. The value of αt decreases markedly with increasing wavelength, indicating strong optical absorption in the shorter-wavelength region and comparatively weak absorption in the visible-to-near-infrared region. To indicate the uncertainty associated with the UV–Visible measurement, error bars were included in the αt values. Assuming an absorbance uncertainty of ±0.005 AU, the corresponding uncertainty in αt was estimated using αt = 2.303A, giving $\Delta(\alpha t) = 2.303\Delta A \approx \pm 0.0115$. The error bars therefore represent the estimated instrumental uncertainty rather than the standard deviation of repeated measurements.

The optical band gap (Figure 7) of the film was found to be of the order 3.32eV which is estimated by the Tauc relation in the case of a direct allowed transition [38],

$$(\alpha h\upsilon)^{\frac{1}{n}} = A\,(h\upsilon - E_g) \qquad (6.2)$$

Where 'α' is absorption coefficient, A is constant, 'hυ' is photon energy and 'Eg' is the optical band gap energy. The exponent 'n' depends on the nature of the transition, n=1/2, 2, 3/2 or 3 for allowed direct, allowed direct, forbidden direct or forbidden indirect transitions, respectively.

4.6 Transmittance Studies

To determine the optical properties and bandgap of aluminium doped zinc oxide thin film UV–visible spectroscopy was carried out (Figure 8). The optical transmittance spectrum of the AZO thin film was obtained in the wavelength range of 300-950 nm. The film was found to have good absorption at the U-V region, and up to 380 nm, the transmittance was less than 6% and increased sharply toward visible region. The optical transmittance increased from 12.47% at 400 nm to 59.29% at 620 nm and reached a maximum value of 80.17% at 640 nm. There was moderate transmittance fluctuation beyond 640nm then the overall increase in transmittance toward the near infra-red region of 79.07% at 950nm. Intrinsic absorption close to the fundamental absorption edge, optical interference phenomenon and scattering due to the surface morphology

ISSN 2278-2540 | DOI: 10.51583/IJLTEMAS | Volume XV, Issue VIII, August 2026

of the AZO film have been found to be associated with these spectral variations. The highest transmittance value obtained was 80.17 ± 0.92%, which is acceptable for TCO applications.

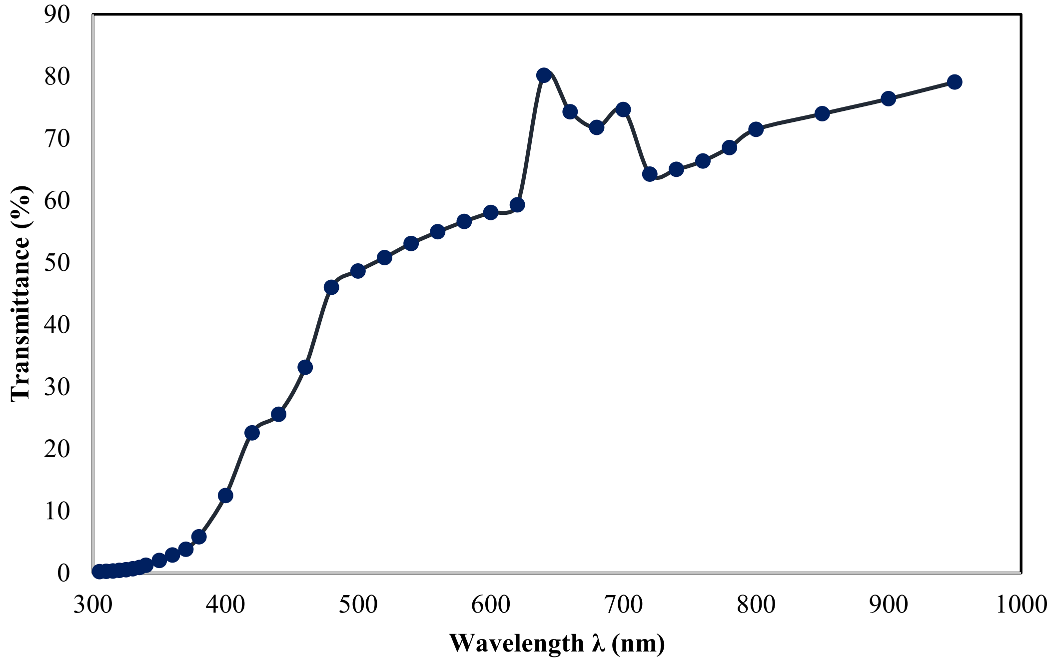

Figure 8: Variation of optical transmittance vs. wavelength of deposited aluminium doped zinc oxide thin films

Error bars are the instrumentally estimated uncertainty obtained by propagating the adopted photometric uncertainty of the UV–Visible spectrophotometer through the absorbance–transmittance relationship. The uncertainty estimation in this case allows us to write the maximum transmittance at 640 nm as 80.17 ± 0.92%.

CONCLUSIONS

To achieve the aluminium-doped zinc oxide (AZO) thin film, the spray pyrolysis technique was successfully used on glass substrates at 573 K. The structural analysis proved that the nanocrystalline AZO phase was formed with a hexagonal wurtzite structure and preferential orientation along the (002) plane. The films had an even, dense granular structure with very few voids. The optical band gap was found as 3.32 eV and the electrical resistivity of it was found as 4.21×10^{-3} Ω cm. High optical transmittance, of the order of 80.17 ± 0.92%, was noticed in the visible region. The excellent optical transparency along with wide band gap and appropriate electrical conductivity indicate that the AZO is a potential indium-free TCO material. Moreover, the process of spray pyrolysis has merits of simple processing, comparatively low equipment price, easy control of deposition parameters and the ability to process on large area substrates, thus suggesting the possibility of using large area substrates for the scalable and cost-effective production of AZO coatings. Therefore, spray-pyrolysed AZO thin films have great potential to be used as transparent electrodes in optoelectronic and other device applications.

REFERENCES

1. Salman, K. A., Omar, K., & Hassan, Z. (2012). Effective conversion efficiency enhancement of solar cell using ZnO/PS antireflection coating layers. Solar Energy, 86(1), 541.
2. Jalali, A., Vaezi, M. R., Naderi, N., Taj Abadi, F., & Eftekhari, A. (2019). Investigating the effect of sol–gel solution concentration on the efficiency of silicon solar cells: role of ZnO nanoparticles as anti-reflective layer. Chemical Papers, 74(1), 253.
3. Jayaraj, M. K., Antony, A., & Ramachandran, M. (2002). Transparent conducting zinc oxide thin film prepared by off-axis rf magnetron sputtering. Bulletin of Mat. Science, 25(3), 227.

ISSN 2278-2540 | DOI: 10.51583/IJLTEMAS | Volume XV, Issue VIII, August 2026

4. Muiva, C. M., Sathiaraj, T. S., & Maabong, K. (2011). Effect of doping concentration on the properties of aluminium doped zinc oxide thin films prepared by spray pyrolysis for transparent electrode applications. Ceramics International, 37(2), 555.
5. Lokesh, K. S., Kumar, J. R. N., Kannantha, V., pinto, T., & Sampreeth, U. (2020). Experimental evaluation of substrate and annealing conditions on ZnO thin films prepared by sol-gel method. Materials Today: Proceedings, 24, 201.
6. Rogers, D. J., Teherani, F. H., Sandana, V. E., & Razeghi, M. (2010). ZnO thin films and nanostructures for emerging optoelectronic applications. In L. A. Eldada & E.-H. Lee (Eds.), SPIE Proceedings. SPIE.
7. Zhang, Y.-H., Mei, Z.-X., Liang, H.-L., & Du, X.-L. (2017). Review of flexible and transparent thin-film transistors based on zinc oxide and related materials. Chinese Physics B, 26(4), 047307.
8. Bae, J.-H., Hwang, J. E., Kim, H. D., Zhang, X., & Park, J. (2014). Analysis of Structural and Electrical Properties of Solution-Processed Zinc Oxide Films for Thin-Film Transistor Application. Molecular Crystals and Liquid Crystals, 600(1), 28.
9. Pearton, S. J., Lim, W. T., Wang, Y. L., Shoo, K., Norton, D. P., Lee, J. W., Ren, F., & Zavada, J. M. (2008). Transparent Thin Film Transistors Based on InZnO for Flexible Electronics. Key Engineering Materials, 380, 99.
10. Park, K., Lee, D., Kim, B., Jeon, H., Lee, N., Whang, D., Lee, H., Kim, Y. J., & Ahn, J. (2010). Stretchable, Transparent Zinc Oxide Thin Film Transistors. Advanced Functional Materials, 20(20), 3577. Portico.
11. Hmar, J. J. L. (2020). Non-volatile resistive switching memory device based on ZnO-graphene oxide embedded in a polymer matrix fabricated on a flexible PET substrate. Microelectronic Engineering, 233, 111436.
12. Zhang, H., Zhao, X., Huang, J., Bai, J., Hou, Y., Wang, C., Wang, S., & Bai, X. (2020). Bistable non-volatile resistive memory devices based on ZnO nanoparticles embedded in polyvinylpyrrolidone. RSC Advances, 10(25), 14662.
13. Navale, S. T., Jadhav, V. V., Tehare, K. K., Sagar, R. U. R., Biswas, C. S., Galluzzi, M., Liang, W., Patil, V. B., Mane, R. S., & Stadler, F. J. (2017). Solid-state synthesis strategy of ZnO nanoparticles for the rapid detection of hazardous Cl2. Sensors and Actuators B: Chemical, 238, 1102.
14. Huang, N., Cheng, Y., Li, H., Zhao, L., He, Z., Zhao, C., Liu, F., & Ding, L. (2019). Selective-detection NO at room temperature on porous ZnO nanostructure by solid-state synthesis method. Journal of Colloid and Interface Science, 556, 640.
15. Jia, X., Fan, H., Afzaal, M., Wu, X., & O'Brien, P. (2011). Solid state synthesis of tin-doped ZnO at room temperature: Characterization and its enhanced gas sensing and photocatalytic properties. Journal of Hazardous Materials, 193, 194.
16. Singh, P., Kumar, A., & Kaur, D. (2008). ZnO nanocrystalline powder synthesized by ultrasonic mist-chemical vapour deposition. Optical Materials, 30(8), 1316-1322.
17. Belkhalfa, H., Ayed, H., Hafdallah, A., Aida, M. S., & Ighil, R. T. (2016). Characterization and studying of ZnO thin films deposited by spray pyrolysis: effect of annealing temperature. Optik, 127(4), 2336-2340.
18. Ali, M. Y., Khan, M. K. R., Karim, A. T., Rahman, M. M., & Kamruzzaman, M. (2020). Effect of Ni doping on structure, morphology and opto-transport properties of spray pyrolised ZnO nano-fiber. Heliyon, 6(3).
19. Cui, M. L., Wu, X. M., Zhuge, L. J., & Meng, Y. D. (2007). Effects of annealing temperature on the structure and photoluminescence properties of ZnO films. Vacuum, 81(7), 899-903.
20. Owoeye, V. A., Ajenifuja, E., Adeoye, A. E., Salau, A. O., Adewinbi, S. A., Akindadelo, A. T., ... & Popoola, A. P. I. (2022). Effect of precursor concentration on corrosion resistance and microstructure of ZnO thin films using spray pyrolysis method. Scientific African, 15, e01073.
21. Kaawash, N. M., Halge, D. I., Narwade, V. N., Alegaonkar, P. S., & Bogle, K. A. (2023). Rationally designed state-of-the-art approach for enhancing the ultraviolet photon detection performance of ZnO thin film. Physica B: Condensed Matter, 648, 414396.
22. Gondal, M. A., Drmosh, Q. A., Yamani, Z. H., & Saleh, T. A. (2009). Synthesis of ZnO2 nanoparticles by laser ablation in liquid and their annealing transformation into ZnO nanoparticles. Applied surface science, 256(1), 298-304.

ISSN 2278-2540 | DOI: 10.51583/IJLTEMAS | Volume XV, Issue VIII, August 2026

23. Kanade, K. G., Kale, B. B., Aiyer, R. C., & Das, B. K. (2006). Effect of solvents on the synthesis of nano-size zinc oxide and its properties. Materials Research Bulletin, 41(3), 590-600.
24. Fang, G. J., Li, D., & Yao, B. L. (2002). Influence of post-deposition annealing on the properties of transparent conductive nanocrystalline ZAO thin films prepared by RF magnetron sputtering with highly conductive ceramic target. Thin solid films, 418(2), 156-162.
25. Jayaraj, M. K., Antony, A., & Ramachandran, M. (2002). Transparent conducting zinc oxide thin film prepared by off-axis rf magnetron sputtering. Bulletin of Materials Science, 25(3), 227-230.
26. Mondal, S., Kanta, K. P., & Mitra, P. (2008). Preparation of Al-doped ZnO (AZO) thin film by SILAR. J. Phy. Sci., 12, 221-229.
27. Chen, K. J., Fang, T. H., Hung, F. Y., Ji, L. W., Chang, S. J., Young, S. J., & Hsiao, Y. J. (2008). The crystallization and physical properties of Al-doped ZnO nanoparticles. Applied surface science, 254(18), 5791-5795.
28. Alaeddine, A., Rachidi, I., Bahsoun, F., Mohanna, Y., Bazzi, O., Hassan, F. E. H., & El-Hadath, B. L. (2009). Influence of Al dopant on the optical and electrical properties of zinc oxide thin films prepared by spray pyrolysis. J Appl Sci, 9(8), 1588-1592.
29. Ismail, A. S., Mamat, M. H., & Mahmood, M. R. (2017). Aluminium-and iron-doped zinc oxide nanorod arrays for humidity sensor applications. Nanostructured Materials-Fabrication to Applications, 9, 167-184.
30. Hjiri, M., El Mir, L., Leonardi, S. G., Pistone, A., Mavilia, L., & Neri, G. (2014). Al-doped ZnO for highly sensitive CO gas sensors. Sensors and Actuators B: Chemical, 196, 413-420.
31. Samoei, V. K., & Jayatissa, A. H. (2020). Aluminum doped zinc oxide (AZO)-based pressure sensor. Sensors and Actuators A: Physical, 303, 111816.
32. Kim, D. S., Park, J. H., Shin, B. K., Moon, K. J., Son, M., Ham, M. H., ... & Myoung, J. M. (2012). Effect of deposition temperature on the properties of Al-doped ZnO films prepared by pulsed DC magnetron sputtering for transparent electrodes in thin-film solar cells. Applied Surface Science, 259, 596-599.
33. Kaid, M. A., & Ashour, A. (2007). Preparation of ZnO-doped Al films by spray pyrolysis technique. Applied surface science, 253(6), 3029-3033.
34. Ambedkar, A. K., Singh, M., Kumar, V., Kumar, V., Singh, B. P., Kumar, A., & Gautam, Y. K. (2020). Structural, optical and thermoelectric properties of Al-doped ZnO thin films prepared by spray pyrolysis. Surfaces and Interfaces, 19, 100504.
35. Hazmin, S. N., Zahid, F. S. S., Sauki, N. S. M., Mamat, M. H., & Amalina, M. N. (2020). The physical and optical properties of AZO thin films on teflon substrate at low deposition temperature by spray pyrolysis. Indonesian Journal of Electrical Engineering and Computer Science, 18(3), 1222-1228.
36. AL-Arique, H. Q., AL-Qadasy, S. S., Kaawash, N. M., Chishty, S. Q., & Bogle, K. A. (2024). Study the characterization of ZnO and AZO films prepared by spray pyrolysis and the effect of annealing temperature. Optical Materials, 150, 115261.
37. Ibrahim, S. G. (2021). Physical properties of chemically spray deposited nanocrystalline manganese sulfide (MnS) thin films. Journal of Materials Science: Materials in Electronics, 32(1), 543-550.
38. Ibrahim, S. G., & Ubale, A. U. (2014). Structural, electrical and optical properties of nanostructured $Cd_{1-x}Fe_xS$ thin films deposited by chemical spray pyrolysis technique. Journal of Molecular Structure, 1076, 291-298.